Regular Article

INORGANIC CHEMISTRY RESEARCH
Published by the
Iranian Chemical Society
www.inorgchemres.org
info@inorgchemres.org

Inorg. Chem. Res., *Vol. 2, No. 2, 95-107, December 2019*
DOI: 10.22036/icr.2019.187495.1050

Interaction of Novel Ni^{2+}, Cu^{2+} and VO^{2+} Complexes of a Tridentate Schiff Base Ligand with DNA, BSA and their Cytotoxic Activity

M. Dostani[a], A.H. Kianfar[a,*], H. Farrokhpour[a], F. Abyar[a], A.A. Momtazi-Borojeni[b,c] and E. Abdollahi[d]

[a]*Department of Chemistry, Isfahan University of Technology, Isfahan, Iran, 84156-83111*

[b]*Nanotechnology Research Center, Bu-Ali Research Institute, Mashhad University of Medical Sciences, Mashhad, Iran*

[c]*Department of Medical Biotechnology, Student Research Committee, Faculty of Medicine, Mashhad University of Medical Sciences, Mashhad, Iran*

[d]*Department of Medical Immunology, Student Research Committee, Faculty of Medicine, Mashhad University of Medical Sciences, Mashhad, Iran*

(Received 30 May 2019, Accepted 1 October 2019)

In this research, the interaction of [CuL(DMF)], [NiL(DMF)] and [VOL(DMF)] (where L = ((E)-4-((2-amino-5-nitrophenylimino)methyl)benzene-1,3-diol)) complexes derived from tridentate Schiff base ligand with bovine serum albumin (BSA) and DNA was investigated *via* electronic absorption and fluorescence spectroscopy. The Ultraviolet-Visible (UV-Vis) spectra exhibited an isosbestic point for the complexes through titration with DNA. The experimental results showed the presence of intercalation interaction between the complexes and calf-thymus DNA (CT-DNA). The interaction of BSA protein and complexes was significant. The recorded florescence spectra of complexes interacting with DNA and BSA revealed the static quenching manner. The free binding energies of complexes and their interaction modes with DNA and BSA were determined by the molecular docking. MTT-dye reduction technique was applied to define cytotoxicity of [NiL(DMF)], [CuL(DMF)] and [VOL(DMF)] complexes against breast cancer 4T1 and colon carcinoma C26 cell lines. The [VOL(DMF)] complex had cytotoxic activity against 4T1 and C26 cell lines.

Keywords: CT-DNA, UV-Vis absorption spectroscopy, Fluorescence spectroscopy, DNA, BSA theoretical studies

INTRODUCTION

Many important applications have been reported for the Schiff base complexes with various structure [1-3]. The biological activites like anticancer, antifangal and antibacterial are on the top these applications [4,5]. Human community cancer is one of the most deadly illnesses. Anti-cancer drugs such as cisplatin and similar compounds have three major problems: (i) these drugs have side and poisonous effects in the body, especially for kidneys, (ii) they are not good drugs for advanced cancer, (iii) finally, they have medicine resistance. Among non platinum drugs, the Schiff base complexes have good interaction with DNA as goal molecule for anti-cancer medicines [6].

The interactions of DNA and Schiff base complexes have been shown through the non covalant (electrostatic, groove binding and intercalation) and covalant bonding [7]. Transfering of drugs into the cancerous tissues generally perform *via* Bovine Serum Albumin (BSA) [8]. Ongoing investigations were done on copper(II) and nickel(II) complexes because of biotic importance in the living systems. Copper(II) and nickel(II) Schiff base complexes with different ligands have unique anticancer properties for cancers such as liver carcinoma cells, pulmonary carcinoma, skin cancer cells and *etc*. [9,10].

Among the used drugs for chemotherapy, attention focused on vanadium Schiff base complexes because of their bioessential properties in living creature that

*Corresponding author. E-mail: akianfar@cc.iut.ac.ir

accountable for many activities. Nowadays, many vanadium combinations prevent from the replication of DNA that shows these compound can be applied as anti-cancer drugs [11].

Here, the interaction of prepared complexes [CuL(DMF)], [NiL(DMF)] [VOL(DMF)] with DNA and BSA was studied theoretically and experimentally. Experimental studies interaction of Schiff base complexes with DNA and BSA were investigated by ultraviolet-visible (UV-Vis), fluorescence spectroscopies, and thermal analysis. Also, cytotoxicity of above complexes against breast cancer 4T1 and colon carcinoma C26 cell lines, as well as normal fibroblast NIH cell line was investigated.

EXPERIMENTAL

Chemicals and Apparatus

All used materials in this paper chemically uncontaminated. Calf thymus DNA (CT-DNA), BSA and methylene blue (MB) were purchased from the Sigma-Aldrich chemical company. Varian Cary 100 UV-Vis spectrophotometer was used for recording the absorption spectra. Cary Eclipse fluorescence spectrophotometer employed for the fluorescence spectra. Mouse breast cancer 4T1 and colon carcinoma C26 cell lines, and normal fibroblast NIH cells were supplied from the National Cell Bank of Pasture Institute, Tehran, Iran.

Synthesis of H_2L and Complexes

The synthesis of ligand (H_2L) and complexes [ML(DMF)] has recently been explained *via* the following process: The tridentate Schiff base ligand (H_2L) was produced *via* reflux of methanolic solution of 4-nitro-1,2-phenylenediamine and 2,4-dihydroxybenzaldehyde in equimolar combination [12]. (H_2L) was dissolved in dimethylformamide (DMF) and then equimolar of salts of Nickel(II) acetate, Copper(II) acetate and Vanadium(IV) oxide acetylacetonate was added to the reaction vessel [12].

[H_2L] Yield (80%). FT-IR (KBr cm^{-1}) ν_{max} 3490 (O-H), 3450, 3380 (NH_2), 1619, (C=N), 1341 (NO_2). UV-Vis, λ_{max} (nm) (DMF): 288, 311 and 391.

[NiL(DMF)] Yield (80%). FT-IR (KBr cm^{-1}) ν_{max} 3369 (NH), 1662 (C=O), 1590 (C=N), 1339 (NO_2). UV-Vis, λ_{max} (nm) (Ethanol): 274, 319, 413.

[VOL(DMF)] Yield (75%). FT-IR (KBr cm^{-1}) ν_{max} 3209 (NH), 1651 (C=O), 1602 (C=N), 1341 (NO_2), 976 (V-O). UV-Vis, λ_{max} (nm) (DMF): 321, 381.

[CuL(DMF)] Yield (85%). FT-IR (KBr cm^{-1}) ν_{max} 3356 (NH), 1660 (C=O), 1599 (C=N), 1341 (NO_2). UV-Vis, λ_{max} (nm) (Ethanol): 271, 341, 432.

DNA Binding Experiments

For all complexes, DNA binding investigation was done in Tris-HCl buffer [5 mM, of 2-amino-2-hydroxymethyl-propane-1,3-diol (Tris) and 50 mM, NaCl, pH 7.3], that used for 72 h reserved at 4 °C. For the characterization of CT-DNA concentrations, the UV-Vis at 260 nm was applied (ε = 6600 l mol^{-1} cm^{-1}) [13]. For UV-Vis absorbance examination, specific quantity of DNA was added to a constant concentration of the complexes. The MB-DNA solution was prepared in buffer solution for the study of fluorescence quenching. For all of the titrations, different amounts of complexes were added to the constant concentration of the MB-DNA solution.

BSA Binding Experiments

The BSA binding studies were done in Tris-HCl buffer at pH = 7.3 in the lab temperature. For recording the UV-Vis spectra, different amounts of complexes were gradually added to determine the BSA concentration. The fluorescence titrations of BSA solutions were completed at the fixed BSA concentration with the various concentrations of the complexes that were documented in the wavelength of 300-450 nm with excitation wavelength of 295 nm.

MTT Assay

Dulbecco's Modified Eagle Medium (DMEM) supplemented with 10% heat-inactivated fetal bovine serum (FBS), 100 U ml^{-1} penicillin, 100 µg ml^{-1} streptomycin and 5 mM *L*-glutamine was used to culture cell lines incubated at 37 °C in a humidified atmosphere containing 5% CO_2. To evaluate the cytotoxicity of [CuL(DMF)], [NiL(DMF)] and [VOL(DMF)] complexes, the MTT [3-(4,5-dimethylthiazol-2-yl)-2,5-diphenyl-tetrazolium bromide] colorimetric assay was employed. The test is based on the metabolic reduction of soluble MTT to insoluble formazan by mitochondrial enzyme activity of viable tumor cells. The insoluble formazan is a colored product that can be

spectrophotometrically quantified after dissolution in dimethyl sulfoxide (DMSO).

To carry out the cytotoxicity assay, 180 µl of cells (5×10^4 cells ml^{-1}) was seeded in 96 wells microplate and incubated in 37 °C, 5% CO_2 air humidified, for 24 h. After that, the attached cells were treated with 20 µl of the prepared concentrations of each compound. Before being added to the culture media, the compounds were dissolved in 0.5% (v/v) DMSO.

Control group was treated with aqueous compound-free containing DMSO at the same concentration [0.5% (v/v)] of treated groups. After 48 h of incubation, 20 µl of MTT solution (5 mg ml^{-1} in phosphate buffer solutions) was added and the plates were incubated for another 3 h. 150 µl of the medium containing MTT were then replaced by DMSO and pipetted to dissolve any formed formazan crystal. Their absorbance was then determined at 560 nm using an ELISA plate reader (Awareness Technology Inc., stat fax 2100). Results were obtained from three independent experiments and each experiment was performed in triplicate. IC_{50} values (concentration that inhibits cell growth by 50%) of the compounds against each tested cell line was calculated using nonlinear regression of concentration-response curves. The selectivity index (SI) was also calculated based on the IC_{50} ratio of normal fibroblast NIH cells and cancer (4T1 and C26) cells. SI value indicates the selectivity of the sample to the tested cell lines. Samples with SI values greater than 2 were considered to have a high selectivity [14].

Computational Methods

Molecular docking. Molecular docking calculation is a theoretically method to find interaction of ligand with receptor, theoretically. The interaction of three complexes ([NiL(DMF)], [CuL(DMF)] and [VOL(DMF)]) with DNA and BSA protein was investigated to blind and focus molecular docking analyses by Auto Dock 4.2 package [15]. The structure of DNA (PDB ID: 423D) with sequence d (ACCGACGTCGGT) 2 and BSA (PDB ID: 4F5S) were taken from the protein data bank [16] (RCSB) with the resolution of 1.60 and 2.47 Å, respectively. The structure of complexes was taken from their X-ray diffraction (XRD) data. On the elementary docking, the blind docking (BD) process was considered for all of docking calculation [17,18]. The BD can help in the prediction of possible binding sites and detects the location of the interaction of a ligand on the entire target surface (DNA and BSA). Finally, a location with the highest binding affinity can be found by the BD calculations. Then, the structures of DNA + complex and BSA + complex, obtained from the BD, were used as initial structures for doing focus molecular docking. The size of the grid map in the focus docking calculations for [NiL(DMF)], [CuL(DMF)] and [VOL(DMF)] complexes with DNA, was set $62 \times 48 \times 56$, $56 \times 58 \times 46$ and $64 \times 58 \times 68$ $Å^3$, along the x, y and z directions, respectively. Similarly, for the focus molecular docking study of BSA with complexes, docking box with dimensions of $96 \times 90 \times 88$, $94 \times 100 \times 100$ and $126 \times 126 \times 126$ $Å^3$ along the *x*, *y* and *z* directions with grid point spacing of 0.375 Å was defined for the program in all of the complexes. The scheme of the residues of the binding site of DNA with Cu, Ni and V complexes has also been generated by LIGPLOT + software [19].

RESULTS AND DISCUSION

Characteristion of Complexes

Based on reported research [12], the Schiff base ligand and complexes were prepared and identified *via* IR spectroscopy. The stretching frequencies of azomethine group -CH=N are moved to lower wavenumbers in the spectra of whole complexes, indicating the coordination of the azomethine nitrogen atom to the metal ions. Also through coordination of DMF to complexes, the IR spectra of compounds showed a different peak correlated to C=O of coordination DMF in the region of 1651-1662 cm^{-1}. Another finger print in the IR spectra of complexes is related to the Stretching frequency of the (V=O) of [VO(DMF)] complex at 976 cm^{-1} [12].

DNA Binding Studies

UV-Vis characteristics of DNA-Schiff base. The affinity of the Schiff base complexes with CT-DNA was studied by UV-Vis spectroscopy to investigate the probable binding types to DNA and define their binding constants (K_b). In the current study absorption titrations were done through variable DNA concentration but in the constant value of complexes. Figure 1 displays the UV-Vis spectra of

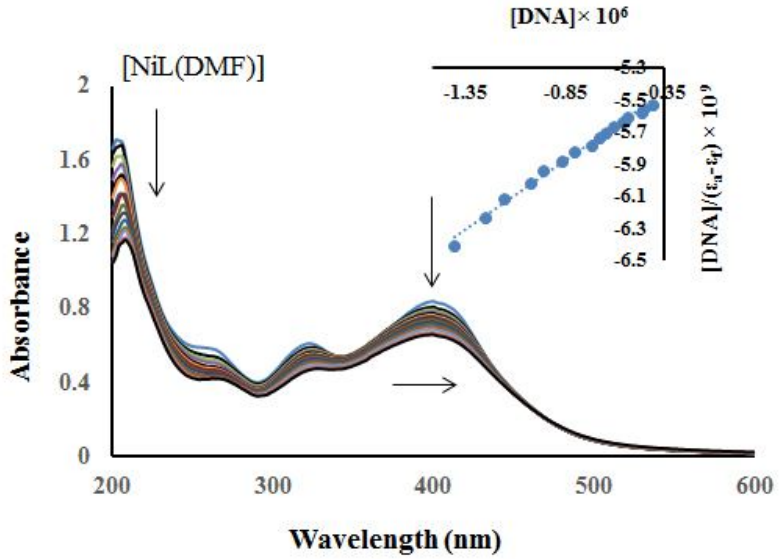

Fig. 1. Electronic spectra of the the [NiL(DMF)] complex in the buffer solution (5 mM TrisHCl/50 mM NaCl at pH 7.4) upon addition of CT-DNA. *C*(complex) = 1.5 × 10^{-5} M, *C*(DNA) = 0- 3 × 10^{-5} M. The arrow displays that the absorption intensities were reduced upon increasing DNA concentration. Inset: Plots of [DNA]/[ε_a - ε_f] *vs*. [DNA] for the titration of complex with DNA.

complexes without or with specified concentrations of DNA. With titrations metal complexes *via* DNA, the absorption spectra of metal complexes show a red shift and a hypochromism [20]. The red-shift into UV-Vis spectra happened througth the strong π-π* stacking contact between DNA base pairs and the aromatic group of the ligand in Schiff base complexes [21]. The value of minor hypochromic for [CuL(DMF)], [NiL(DMF)] and [VOL(DMF)] complexes are 10.3, 13.1 and 14.6%, respectively where calculated through Eq. (1) [22].

$$H\% = (A_{Free} - A_{bounded}) / A_{Free} \times 100 \quad (1)$$

Additional study of the binding strength of the small molecules with DNA obtained by intrinsic binding constant (K_b) that calculated by Eq. (2) [23].

$$\frac{[DNA]}{(\varepsilon_a - \varepsilon_f)} = \frac{[DNA]}{(\varepsilon_b - \varepsilon_f)} + \frac{1}{K_b\,(\varepsilon_b - \varepsilon_f)} \quad (2)$$

In this equation [DNA] is the concentration of DNA in base pairs, the absorption coefficient ε_a, ε_f, and ε_b correspond to A_{obs}/[DNA], the extinction coefficient of the free compound and the extinction coefficient of the compound when entirely bound to DNA, respectively. In Fig. 1, S1 and S2 (inset) the plot of [DNA]/[ε_a - ε_f] *vs*. [DNA] provides straight line with the intercept $1/K_b[\varepsilon_b - \varepsilon_f]$ and the slope $1/[\varepsilon_a - \varepsilon_f]$ when the number of data put into Eq. (2). The ratio of the slope to the intercept gives (K_b) for [CuL(DMF)], [NiL(DMF)] and [VOL(DMF)] complexes the K_b values are 4 × 10^{-5}, 5.3 × 10^{-5} and 7.2 × 10^{-5} M^{-1}, respectively. This value of K_b is similar to a typical intercalator for instance EtBr (K_b = 1.5 × 10^{-5} M^{-1}) that represents interaction among Schiff base complexes and DNA is intercalative style. Moreover, isosbestic point is observed in the UV-Vis spectra of [CuL(DMF)] and [VOL(DMF)]. The existence of isosbestic points in the absorption spectra indicates that there is equilibrium among concentration of small molecules in free mode and connected made to DNA that shows the binding mode among the complexes and DNA is intercalation [24].

With binding constant (K_b), the values of the free energy (ΔG) was calculated. Free energy (ΔG) was used for study the spontantaneous/non-spontantaneous of small molecules-DNA that occurred with Eq. (3) [25].

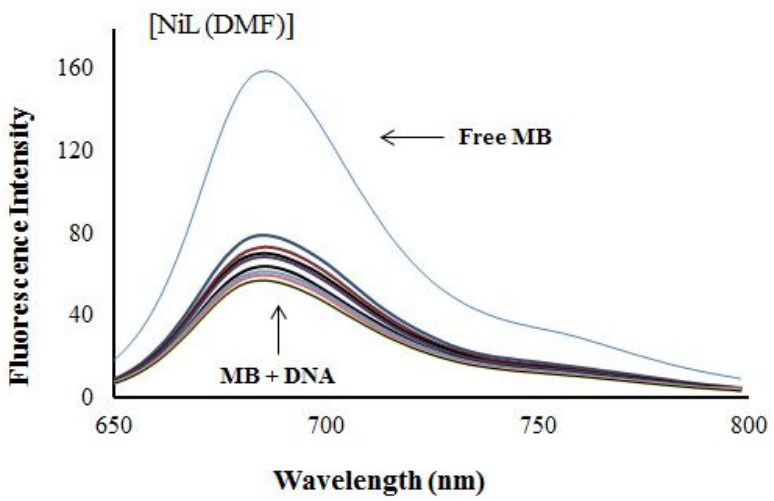

Fig. 2. The emission spectra of the DNA-MB system, in the existence of [NiL(DMF)] complex, *C*(DNA) = 5 × 10^5 M , *C*(complex) = 0-2.5 × 10^{-5} M, *C*(MB) = 5 × 10^{-6} M. The arrow displays the emission intensity variations upon increasing complex concentration. The inserts correspond to the molecular structures of methylene blue.

$$\Delta G_b = - RT\ln K_b \quad (3)$$

The calculated ΔG_b for [CuL(DMF)], [NiL(DMF)] and [VOL(DMF)] complexes are -7.89, -6.46 and 8.03 kcal mol^{-1}, respectively , that represents the spontaneity of DNA-compound interaction.

Fluorescence studies: Competitive interaction of complex with MB-DNA. Methylene blue (MB) was used to explore the possible DNA binding method of the Ni(II), Cu(II) and VO(IV) complexes. MB released intense fluorescence at 685 nm in the absence of DNA duplex. When MB intercalated to DNA, the intense fluorescence was decreased. The intensity of fluorescence spectra of solutions was increased with adding of different complexes of [CuL(DMF)], [NiL(DMF)] and [VOL(DMF)] to the DNA-MB. In performed measurements in environment temperature, complexes did not show luminescence. It was determined that MB was a good DNA intercalator with poor fluorescent because of DNA-MB interaction. Fluorescence spectra for [CuL(DMF)], [NiL(DMF)] and [VOL(DMF)] are presented in Fig. 2. As it can be seen in Fig. 2, S3 and S4 when various concentrations of the small molecules were added to DNA-MB system, the fluorescence intensity was increased. The fluorescence quenching explains that complexes can substitute the intercalated MB to DNA. Also, the complexes were interacted to DNA with the intercalative type [26].

BAS Binding Studies

Absorption spectral studies. UV-Vis analysis was applied as a simple technique to identify the essential variations and interactions of the complex with BSA. The UV-Vis absorption spectra of BSA were collected without and with of different amounts of complexes. With adding the [NiL(DMF)], [VOL(DMF)] and [CuL(DMF)] complexes (Fig. 3, S5, S6), the intensity of BSA absorption peak at about of 208-240 nm, which was produced from $\pi \rightarrow \pi^*$ transition of the strength polypeptide building, visibly reduced and the peak shifted somewhat toward longer wavelength owing to the perturbation of the secondary arrangement of the protein [27]. The UV analysis showed a weak band of BSA at around 278 nm, which was due to the gradual decrease of aromatic amino acids (Phe, Tyr and Trp) [28], although the place of the peak does not change. These clarifications demonstrate that the communication of BSA with the complexes is accomplished.

Tryptophan quenching investigation. Fluorescence

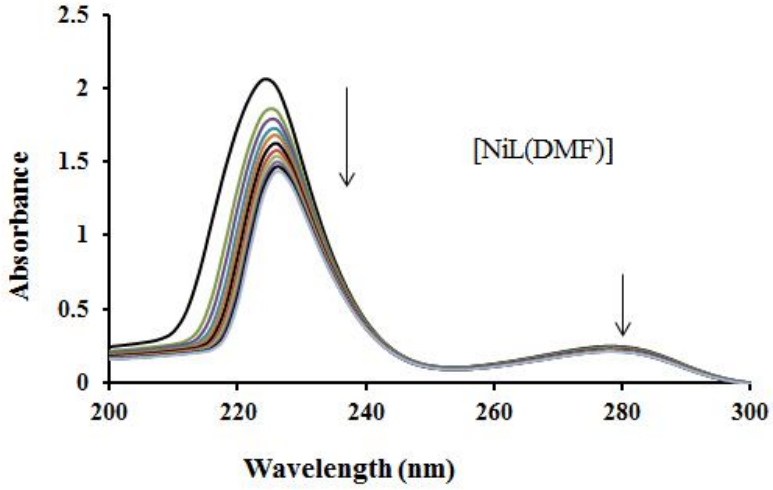

Fig. 3. UV absorption spectra of *C*(BSA) = 3 × 10^{-6} M in the absence and presence of [NiL(DMF)] complex (complex) = 0-4.5 × 10^{-6} M in the 5 Mm Tris-HCl with the 50 Mm NaCl.

investigations are done to observe whether the Ni(II), VO(IV) and Cu(II) complexes interaction with protein is present or absent. The emission spectra of protein without and with small molecules are presented in Fig. 4, S7 and S8. Commonly, among the amino acids of BSA protein three amino acids (tyrosine, tryptophan, and phenylalanine) have good fluorescence characteristics [29]. In the fluorescence spectra, the decreasing of the intense emission band about 342 nm in the inherent fluorescence of protein reflects the interaction between compound and protein [30]. To distinguish the form of quenching mechanism, the Stern-Volmer equation can be applied (Eq. (4)) [29].

$$I_0/I = 1 + K_{sv}[Q] = 1 + K_q\tau_0[Q] \quad (4)$$

In this Eq., I_0 is the fluorescence intensity of protein; I is the reduced intensity of the BSA in the presence of the small molecule (quencher); Q is the quencher, K_{SV} is dynamic quenching constant, K_q is quenching rate constant of the protein and τ_0 is normal lifetime of the biomolecule without quencher. To define $K_{sv,}$ the plot of (F_0/F) against [Q] was drawn. According to the Eq. (4), the obtained value of K_{sv} for different complexes of [CuL(DMF)], [NiL(DMF)] and [VOL(DMF)] were 1.2 × 10^{-5}, 3.1 × 10^{-5} and 1.3 × 10^{-5} M^{-1} s^{-1}, respectively. Base on the conclusions of K_{sv} the quenching capacity of [NiL(DMF)] complex was more than other complexes.

The amounts of K_q for [CuL(DMF)], [NiL(DMF)] and [VOL(DMF)] were calculated 6.49 × 10^{12}, 1.6 × 10^{13} and 6.56 × 10^{12} M^{-1} s^{-1}, respectively. Since the fluorescence lifetime of protein was taken 10^{-8} s, the quenching rate constant, (K_q) was calculated through Eq. (5) [31]:

$$K_q = K_{sv}/\tau_0 \quad (5)$$

K_q for abundant kinds of quenchers to BSA is 2 × 10^{10} l mol^{-1} s^{-1} that is less than the K_q of the [CuL(DMF)], [NiL(DMF)] and [VOL(DMF)] complexes [32]. The amounts of quenching constant demonstrate that the complex between BSA and small molecule is formed and quenching mechanism is static [30].

We used Scatchard Eq. (6) when the static quenching interaction was occurred [33]:

$$\log\frac{(I_0 - I)}{I} = \log K_{bin} + n\log[Q] \quad (6)$$

Where I_0 and I are the similar to them in Eq. (4), K_b is the binding constant for the complex-protein interaction and n is the number of the binding sites per BSA. The K_b quantity of [CuL(DMF)], [NiL(DMF)] and [VOL(DMF)] are 1.2 × 10^5, 3.2 × 10^5 and 1.8 × 10^5 M^{-1}, respectively, that obtained

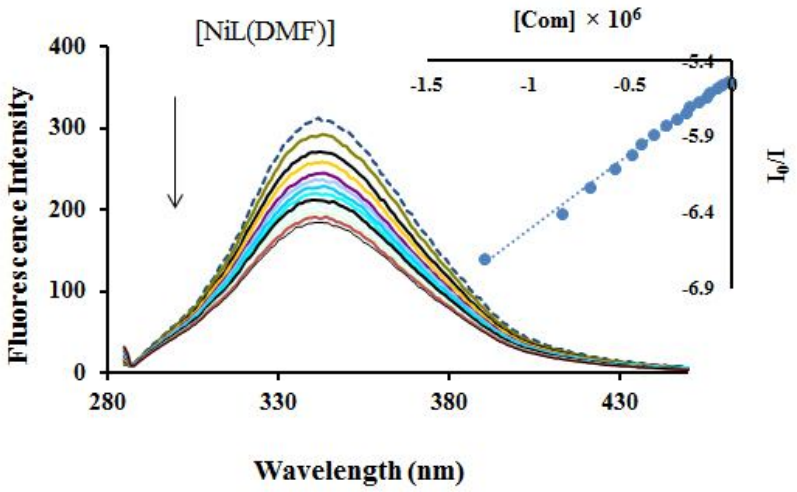

Fig. 4. Emission spectra of BSA upon the titration of [NiL(DMF)] complex. *C*(BSA) = 4×10^{-6} M, *C*(complex) = 0, 4×10^{-6} M. The arrow shows the change upon increasing complex concentration. Inset: Plots of F_0/F *vs*. (complex) for the titration of the complex to BSA.

from the plot of log [I_0 - I/I] *vs*. log[complex]. According to the binding constant quantity [NiL(DMF)] complexes have the strongest connection with BSA. Moreover, the n values for [CuL(DMF)], [NiL(DMF)] and [VOL(DMF)] complexes are 0.7, 1.09 and 0.9, respectively. n < 1 or n = 1 for BSA-complexes suggests merely a binding site per protein [34].

In Vitro Cytotoxic Activity

MTT-dye reduction method, as standard bioassay, was employed to determine cytotoxicity of [NiL(DMF)], [CuL(DMF)] and [VOL(DMF)] complexes against breast cancer 4T1 and colon carcinoma C26 cell lines, as well as normal fibroblast NIH cell line. The cytotoxic activity of cisplatin, as standard reference, was evaluated for comparison purposes. As demonstrated in Fig. 5, all of the complexes showed cytotoxic activity in concentration-dependent manner on both 4T1 and C26 cancer cell lines, and with less extent on the normal NIH cell line. [NiL(DMF)], [CuL(DMF)] and [VOL(DMF)] complexes at the concentrations ranged from 6 to 100 µM showed 13.25%-96.84%, 10.45%-93.25%, and 12.6%-96.9% cytotoxicity, respectively, against 4T1 cancer cells. In the case of C26 cancer cells, at the same concentrations, [NiL(DMF)], [CuL(DMF)] and [VOL(DMF)] complexes exerted 7.4%-99.84%, 19.84%-97.16%, and 12.9%-96.3% cytotoxicity, respectively. The results revealed that [VOL(DMF)] complex can exert high and significant cytotoxic activity with IC_{50} values of 18.49 µM and 20.98 µM against 4T1 and C26 cell lines, respectively. The [NiL(DMF)] and [CuL(DMF)] complexes were also found to have appreciable cytotoxicity with IC_{50} values of (41.23 µM and 67.38 µM) and (33.94 µM and 44.77 µM) against 4T1 and C26 cell lines, respectively. Although, complexes were found to be significantly and highly cytotoxic against both 4T1 and C26 cancer cells, there were low cytotoxicity against NIH normal cells in compared with cisplatin (Table 1). Furthermore, as mentioned in Table 1, the value of SI for the [VOL(DMF)] complex is found to be higher than 2, which it confirms the importance of this sample to be considered as a selective cytotoxic agent against tumor cells.

Molecular Docking of the Complexes with DNA and BSA

Finally, the lowest binding free energy (ΔG^o_b) for the interaction of [NiL(DMF)], [CuL(DMF)] and [VOL(DMF)] complexes with DNA are -7.8, -6.7 and -7.3 kcal mol^{-1} respectively. The active site of DNA in the interaction with complexes is shown in Figs. 6, S9 and S10. The molecular

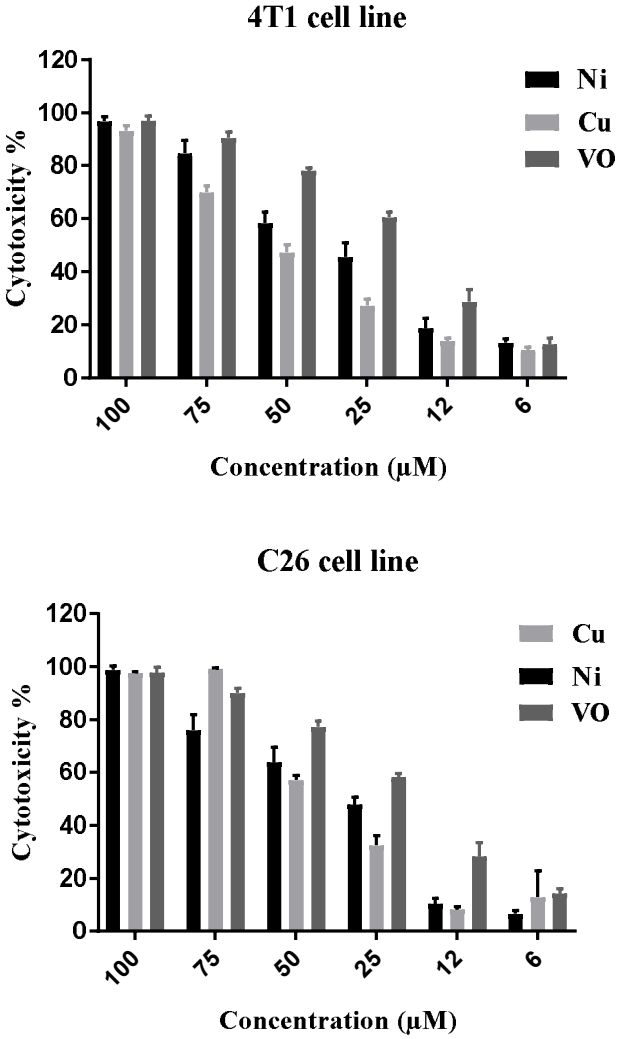

Fig. 5. Concentration-dependent cytotoxic activity of Ni, Cu and VO complexes against 4T1 and C26 cancer cell lines at the concentrations of 6, 12, 25, 50 and 100 µM. The results are the mean ± SD of three independent experiments. All data are significant differences from untreated control by $p < 0.05$.

docking and the binding site s of [NiL(DMF)], [CuL(DMF)] and [VOL(DMF)] complexes interacted with DNA have been shown in the Figs. 6, S9 and S10, respectively. In addition, Figs. 6b, S9b and S10b show the bases of DNA which have dominant interactions with the complex in the interaction region. Figures 7, S11, S12 show the interaction scheme of the residues of the binding site of DNA with [NiL(DMF)], [CuL(DMF)] and [VOL(DMF)] complexes generated by LIGPLOT + software. The dominant interactions between the complexes and residues in the active site with the hydrogen bonds are clearly shown. The K_b amount of [CuL(DMF)], [NiL(DMF)] and [VOL(DMF)] complexes with DNA are 5.5×10^5, 4.5×10^4 and 2.4×10^5 M^{-1}, respectively.

Figures 8, S13 and S14 show docking pose calculated by molecular docking software between BSA and [NiL(DMF)], [CuL(DMF)] and [VOL(DMF)] complexes. The lowest binding site free energy (ΔG^o_b) of the [NiL(DMF)] complex to the BSA -7 kcal mol^{-1} was predicted. In addition, the obtained distances of Trp-134 and

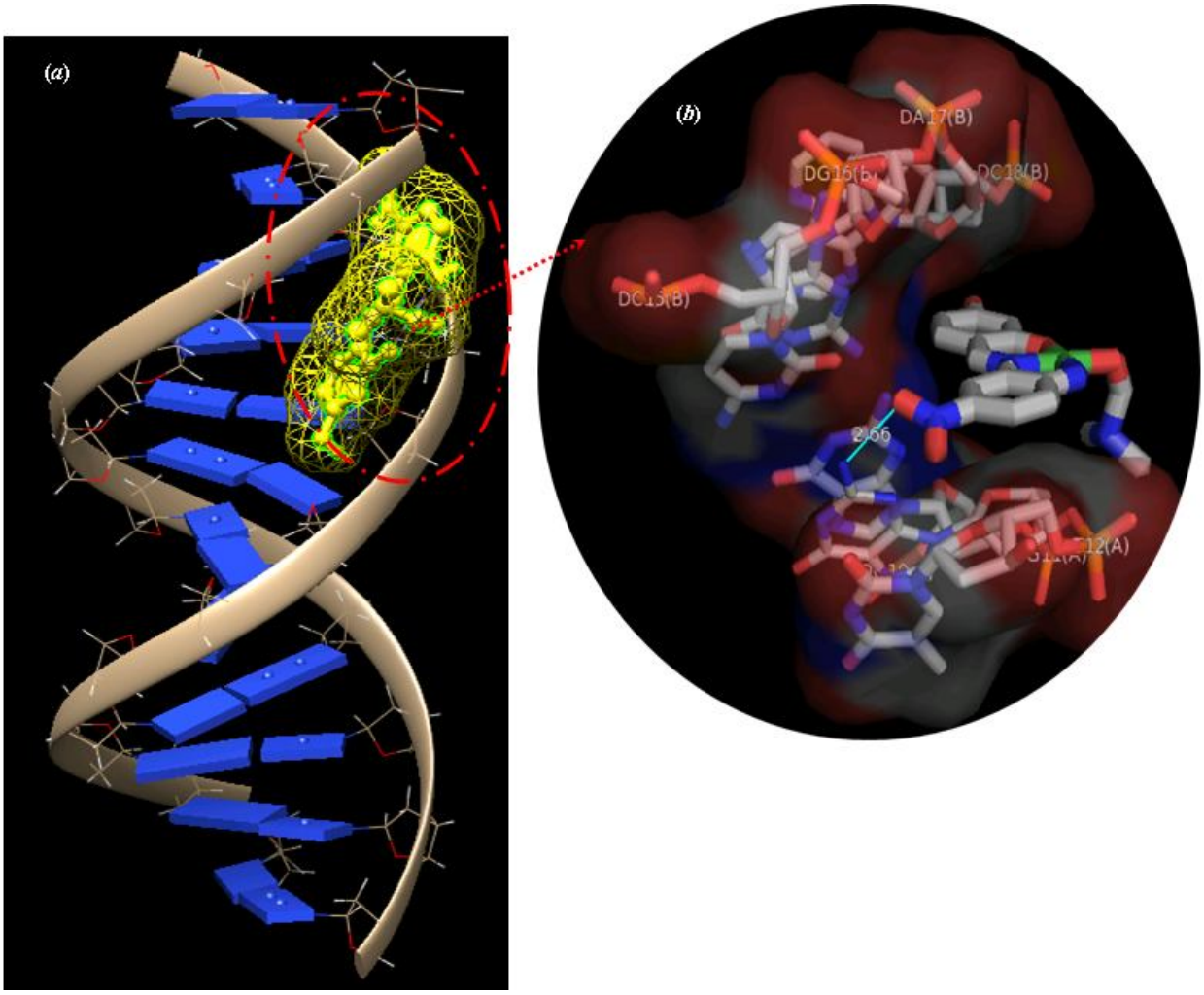

Fig. 6. (a) The [NiL(DMF)] complex is docked in the active site of DNA. (b) The bases of DNA with dominant interactions with the [NiL(DMF)] complex in the active site of the three hydrogen bands are displayed among the complex and bases of DNA.

Trp-231 with [NiL(DMF)] complex were 21.6 and 18.1 Å, respectively. In addition, the hydrophobic interaction residues and hydrogen bonds of protein with [NiL(DMF)] complex were shown in schematic representation of the 2-D in Fig. 9.

Also, there were two hydrogen bonds between [NiL(DMF)] complex and the BSA amino acids. These hydrogen bonds were between [NiL(DMF)] complex with Arg 435 and His 145 residues (with the bond length of 2.8 and 2.94 Å) (see Fig. 9).

The binding mode and intermolecular interaction of the [CuL(DMF)] complex with BSA were shown in Fig. S13. The lowest calculated binding free energy (ΔG^0_b) of the [CuL(DMF)] complex with BSA was -8.9 kcal mol^{-1}. The distances between tryptophan and the [CuL(DMF)] complex obtained from the docking simulation, were 15.8 and 19.5 Å from Trp-134 and Trp-213, respectively.

Figure 15 shows the 2-D interaction of the [CuL(DMF)] complex docked into the binding site of the BSA protein generated by LIGPLOT + software. There are three hydrogen bonds between the [CuL(DMF)] complex with Glu 424, His 145 and Arg 435 amino acids of BSA.

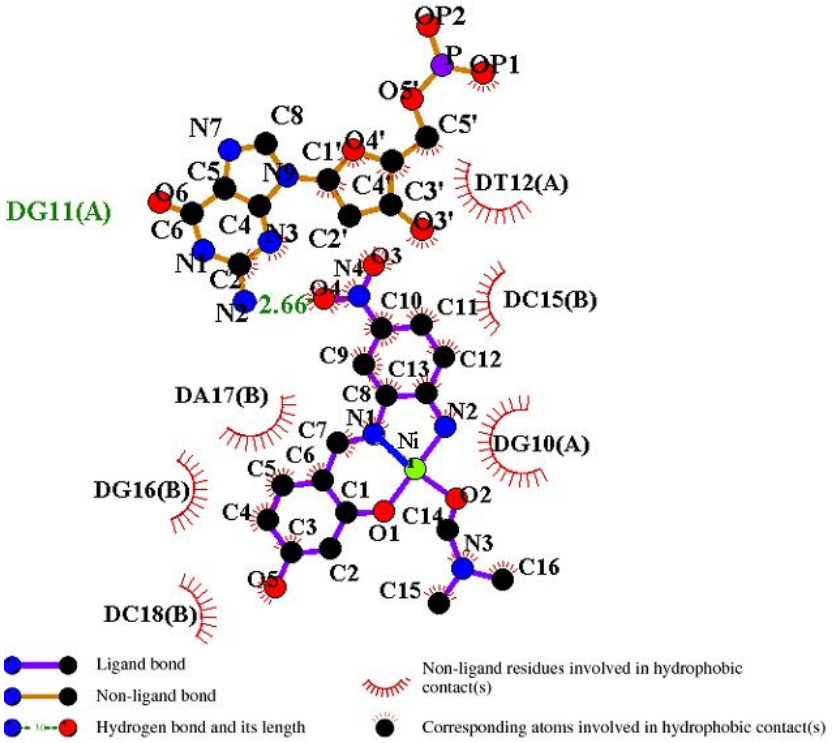

Fig. 7. Schematic representation of hydrophobic interaction and hydrogen bonding of [NiL(DMF)] complex with DNA.

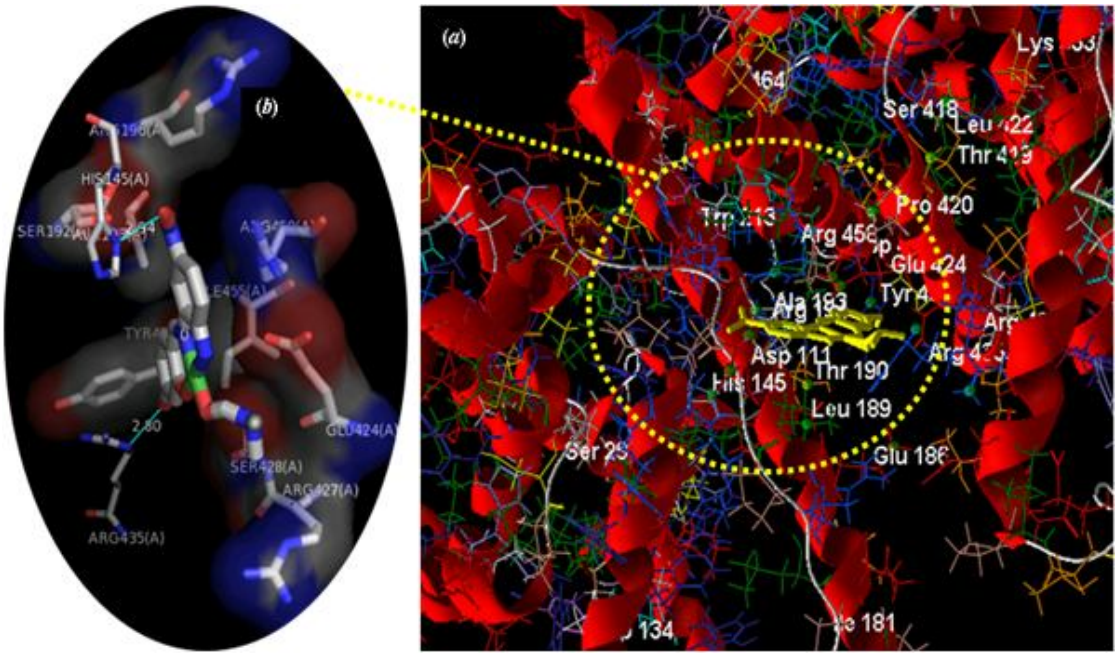

Fig. 8. (a) The residues of BSA interacting with [NiL(DMF)] complex. Trp-134 and Trp-213 have been displayed obviously. The chief residues of BSA interacting with [NiL(DMF)] complex are presented in Fig. 8b.

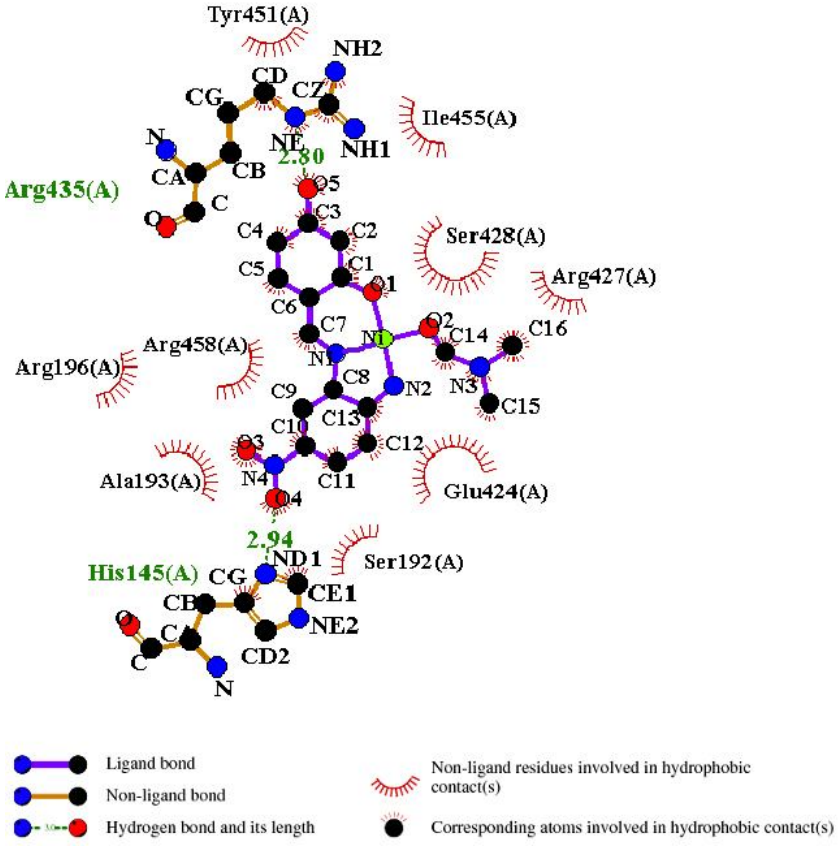

Fig. 9. Schematic representation of the 2-D interactions of the [NiL(DMF)] complex with BSA generated by LIGPLOT+.

The interaction of [VOL(DMF)] complex with BSA protein is shown in Fig. S14, also, the residues of the protein interacted with the [VOL(DMF)] complex at the binding site are mentioned in Fig. S14b. The minimum energy of interaction of [VOL(DMF)] complex with the active site of BSA is (ΔG^{o}_{b}) -6.3 kcal mol^{-1}. Figure S16 shows the 2D schemes of the interaction between the [VOL(DMF)] complex and BSA generated by LIGPLOT+ software. As seen, there are three hydrogen bonds between the [VOL(DMF)] complex and Ser 104, Asp 108 and Lys 204 residues with bond lengths of 2.97, 3.30 and 2.51 Å, respectively. As can be seen, there are hydrophobic and hydrogen interaction between [VOL(DMF)] complex with BSA. The calculated distances of Trp-213 and Trp-134 with the [VOL(DMF)] complex are 19.4 and 22.4 Å, respectively. The amount of K_b for [CuL(DMF)], [NiL(DMF)] and [VOL(DMF)] complexes with BSA is 3.5 $\times 10^{6}$, 1.4×10^{5} and 4.3×10^{4} M^{-1}, respectively.

CONCLUSIONS

The current contribution defines the interaction of [NiL(DMF)], [CuL(DMF)] and [VOL(DMF)] small molecules with DNA and BSA macromolecules. UV-Vis and competitive studies with MB designate that the complexes can mainly connect to DNA with intercalation mode. The BSA-binding studies discovere that three complexes bind to BSA for quenching of tryptophan fluorescence through the static quenching mechanism. Furthermore, the cytotoxic activities of these complexes are done against breast cancer 4T1 and colon carcinoma C26 cell lines. The results show that [VOL(DMF)] complex can significantly improve the cytotoxic activity against 4T1 and C26 cell lines.

Table 1. Selective-cytotoxicity of the Complexes against Different Cancer and Normal Cell Lines

Cell line	Compound	IC50 (μM)	SI
4T1	[VOL(DMF)]	18.49	7.03
	[NiL(DMF)]	41.23	2.2
	[CuL(DMF)]	67.38	1.8
	Cisplatin	12.3	0.85
C26	[VOL(DMF)]	20.98	6.19
	[NiL(DMF)]	33.94	2.68
	[CuL(DMF)]	44.77	2.7
	Cisplatin	8.3	1.26
NIH	[VOL(DMF)]	130	-
	[NiL(DMF)]	91	-
	[CuL(DMF)]	121	
	Cisplatin	10.5	-

ACKNOWLEDGEMENTS

This study was funded and supported by Isfahan University of Technology.

REFERENCE

[1] Y. Li, Z. Yang, M. Zhou, J. He, X. Wang, Y. Wu, Z. Wang, J. Mol. Struct. 1130 (2017) 818.

[2] N. Yılmaz Baran, T. Baran, A. Mentes, Appl. Catal. A. 531 (2017) 36.

[3] L. Ding, Y. Zhang, X. Chen, X. Lü, Inorg. Chem. Commun. 76 (2017) 100.

[4] G. Kalaiarasi, R. Jain, H. Puschman, S.P. Chandrika, K. Preethi, R. Prabhakaran, New J. Chem. 41 (2017) 2543.

[5] M.P. Kesavan, G.G. Vinoth Kumar, J. DhaveethuRaja, K. Anitha, S. Karthikeyan, J. Rajesh, J. Photochem. Photobiol., B: Biology 167 (2017) 20.

[6] N.Z. Li, H. Li, X. Li, J. Dou, S.Wang, RSC Adv. 5 (2015) 37085.

[7] S.P. Dash, A.K. Panda, S. Dhaka, S. Pasayat, A. Biswas, M.R. Maurya, P.K. Majhi, A. Crochet, R. Dinda, Dalton Transactions 45 (2016) 18292.

[8] M. Niu, M. Hong, G.Chang, X. Li, Z. Li, J. Photochem. Photobiol. B. 148 (2015) 232.

[9] A. Terenzi, M. Fanelli, G. Ambrosi, S. Amatori, V. Fusi, L. Giorgi, V.T. Liveria, G. Barone, Dalton Transication 41 (2012) 4389.

[10] P. Li, M. Niu, M. Hong, S. Cheng, J.M. Dou, J. Inorg. Biochemistry 137 (2014) 101.

[11] S.P. Dash, A.K. Panda, S. Pasayat, S. Majumder, A.

Biswas, W. Kaminsky, S. Mukhopadhyay, S.K. Bhutia, R. Dinda, J. Inorg. Biochem. 144 (2015) 1.

[12] A.H. Kianfar, M. Dostani J. Mater. Sci.: Mater. In Electron. 28 (2017) 7353.

[13] S.M. Kumar, K. Dhahagani, J. Rajesh, K. Nehru, J. Annaraj, G. Chakkaravarthi, G. Rajagopal, Polyhedron 59 (2013) 58.

[14] A. Koch, P. Tamez, J. Pezzuto, D. Soejarto, J. Ethnopharmacol. 101(1) (2005) 95.

[15] H. Park, J. Lee, S. Lee, Proteins: Struct. Funct. Bioinf. 65 (2006) 549.

[16] http://www.rcsb.org.

[17] Hetényi, D. van der Spoel., FEBS Lett. 580 (2006) 1447.

[18] Hetényi C, van der Spoel D. Protein Science : A Publication of the Protein Society. 20 (2011) 880.

[19] A.C. Wallace, R.A. Laskowski, J.M. Thornton, Protein Eng. 8 (1995) 127.

[20] R. Fekri, M. Salehi, A. Asadi, M. Kubicki, Polyhedron 1059 (2014) 299.

[21] M. Sedighipoor, A.H. Kianfar, W.A. Kamil Mahmood, M.H. Azarian, Polyhedron 46 (2014) 145.

[22] Q. Guo, L. Li, J. Dong, H. Liu, T. Xu, J. Li, Spectrochim. Acta Part A: Molecular and Biomol. Spectroscopy 106 (2013) 155.

[23] R. Esteghamat-Panah, H. Hadadzadeh, H. Farrokhpour, M. Mortazavi, Z. Amirghofran, Inorg. Chimica Acta 41 (2006) 393.

[24] A. Blake, A.R. Peacocke, Biopolymers 5 (1967) 871.

[25] L.H. Abdel-Rahman, R.M. El-Khatib, L.A.E. Nassr, A.M. Abu-Dief, J. Mol. Struct. 1040 (2013) 9.

[26] N. Nanjundan, P. Selvakumar, R. Narayanasamy, R. A. Haque, K. Velmurugan, R. Nandhakumar, T. Silambarasan, R. Dhandapani, J. Photochem. Photobiol. B: Biology 31 (2012) 294.

[27] F. Arjmand, A. Jamsheera, M. Afzal, S. Tabassum, Chirality 24 (2012) 977.

[28] P. Sathyadevi, P. Krishnamoorthy, E. Jayanthi, R. R. Butorac, A.H. Cowley, N. Dharmaraj, Inorg. Chim. Acta 384 (2012) 83.

[29] P. Li, M.J. Niu, M. Hong, S. Cheng, J.M. Dou, J. Inorg. Biochem. 8 (2003) 626.

[30] L. Andrezálová, J. Plšíková, J. Janočková, K. Koňariková, I. Žitňanová, M. Kohútová, M. Kožurková, J. Organometallic Chem. 827 (2017) 67.

[31] M. Dakovic', H. Cicak, Z. Soldin, V. Tralic-Kulenovic, J. Mol. Struct. 938 (2009) 125.

[32] V. Uma, M. Kanthimathi, T. Weyhermuller, B.U. Nair, J. Inorg. Biochem. 99 (2005) 2299.

[33] Q. Zhou, P. Yang, Inorg. Chim. Acta 359 (2006) 1200.

[34] Y. Li, Y. Wu, J. Zhao, P. Yang, J. Inorg. Biochem. 101 (2007) 283.